A LOW COST OPEN-AIR TRACKING SYSTEM BASED ON AN EMPIRICAL PATH-LOSS MODEL.

Kayla Niu, Asif Shahidullah, Andrea Vilarasau, James Ringle, Michaelina Sorrell, and Luke Zurmehly[1]

Faculty Advisors: Michael W. Marcellin and Kathleen Melde

Department of Electrical and Computer Engineering
The University of Arizona, Tucson, AZ 85721

ABSTRACT

Tracking small marmosets over a large area represents a significant challenge for researchers. The native habitat for such animals are generally unsuitable for GPS based location systems, and the size of the animals prevents large, feature-rich collars from being utilized. Additionally, costs and feasibility prevent researchers from continuously monitoring these animals on the ground. This paper proposes a new system of tracking that offsets complexity from the collar onto fixed Base Stations (BS). The simplified collars emit a ping that multiple BSs then log along with the power of the signal. Combining the data from different BSs allows for the determination of the Signal of Interest (SOI). It was found that using three BSs provided enough accuracy to determine the location of an SOI within an accuracy of 2 m^2 over a roughly 450 m^2 area.

Keywords: geolocation**,** path loss, trilateration, tracking, telemetry

INTRODUCTION

The Golden Lion Tamarin (GLT), native to the coastal Serra do Mar Atlantic forest of Brazil, is classified as an endangered species by the International Union for Conservation of Nature (IUCN). The wild population is now managed by the Save the Golden Lion Tamarin (SGLT) organization,

[1] K. Niu, A. Shahidullah, and A. Vilarasau contributed equally to this work.

working with a network of 150 zoos and 500 captive individuals. Despite the successful conservation initiative, social awareness of the GLT remains low due to its geographic location. Funding for the SGLT conservation program remains low, relative to the cost for equipment and personnel, due to the challenging terrain of the native habitat. SGLT spends $12,000 per year to replace tracking collars used by the researchers, where each collar has a unit price of $200, permitting the researchers to track only two members of each family unit. Usually, the program opts to purchase refurbished collars to minimize recurring costs.

The tracking collars used by the researchers have a six month lifespan, but concerns have been raised regarding the dimensions and weight, since interference with the GLT behavior would invalidate research data. Other products, while more suitable in terms of dimension and weight, rely on GPS; collecting data from these collars, and the availability of a reliable GPS signal deep under the forest canopy prevent the use of these more suitable products. Cost and battery life of these smaller tracking collars are also problematic for the SGLT budget.

The design proposed is a proof-of-concept for tracking multiple collars in a fixed geographic location over an extended period of time using a method that offsets the complexity from the collars onto fixed receiver stations. The system will be constructed such that multiple receiver stations laid out to cover a fixed region will collect the data. This data will be stored at each station and can later be retrieved and processed to calculate the location of the individual collars.

The system will not be constructed for operation in the native environment of the GLT, but it will demonstrate that the technique used to calculate the method is viable. The operational limitations of the environment, such as power limitations, packaging and mounting considerations, and synchronization issues will be implemented in the construction with the final design.

SYSTEM OVERVIEW

Figure 1 shows a graphical representation of the overall system. Three BSs are located in a geographically distributed area so that the collars can be located within the area the base stations cover. In the case of Figure 1, a triangle where the vertices are the BSs would be the maximum area that a SOI can be located in. The BSs store data internally allowing researchers to retrieve data during maintenance cycles. The collars worn by the marmoset, in addition to the BS, are the two main subsystems of the tracking system. The Collar Subsystem transmits a radio signal at 154.570 MHz with a 20 kHz bandwidth that can be detected by at least three receiver stations simultaneously. The information being transmitted derives include a sequence number, a unique ID, pseudorandom number (utilizing the ID as a seed) and a battery status field. The collar subsystem emits a Gaussian Frequency Shift Key (GFSK) modulated waveform at a variable

period in order to maximize battery life.

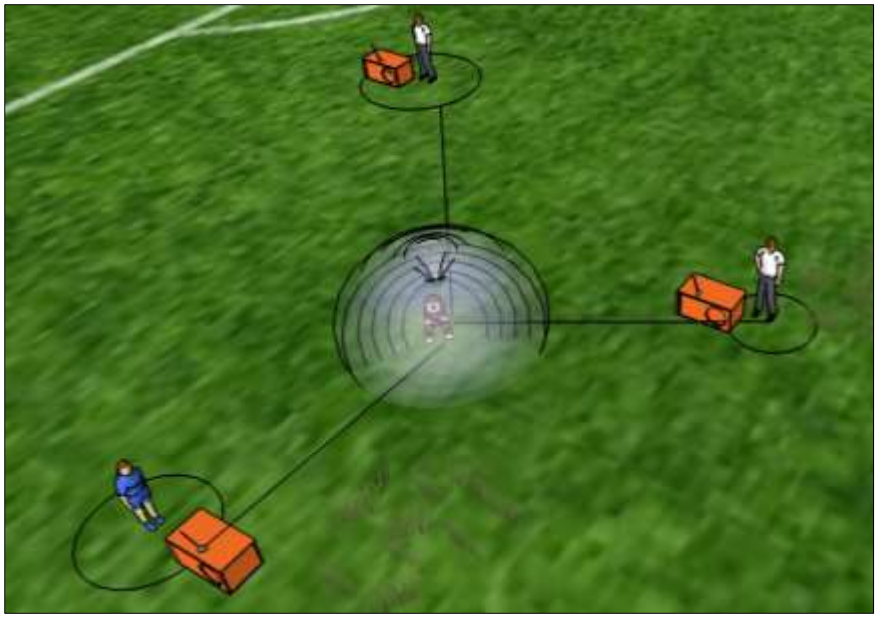

FIGURE 1: GRAPHICAL REPRESENTATION OF THE SYSTEM SHOWING THE LOCATION OF THE BASE STATIONS IN RELATION TO THE SOI.

An empirical radio propagation model, which is developed by profiling the received power of the collar at known distances, is used by the BSs to estimate the distance between itself and the SOI. The data generated by profiling step is curve-fitted using exponential regression, and the inverse of this equation allows for an estimation of distance as a function of power. Profiling and averaging a large number of points results in a more accurate model.

Utilizing multiple BSs gives an element of redundancy to the data, allowing SOIs to be located if the signal did not reach all BSs. Additionally, multiple BSs increases the effective range of the tracking system.

To gauge the location of the collar, power and distance data, stored at each station in the receiver network, is collected manually. Using the estimated distances, a circle with a radius of the estimated distance is drawn out from each respective BS. The intersecting region of these circles represents the estimated location of the target in relation to the network.

ANALYSIS

The method that the system employed was to locate the SOI was trilateration, using at least three fixed BSs as reference points. Trilateration uses the distance between the SOI and reference points to estimate the location of the SOI. Using three reference points allows for a location to be determined within a 2D plane.

The distance was estimated using a radio propagation, or path-loss, model. The loss of power of an electromagnetic wave as it propagates through space is what is used to estimate the distance from the observation point to the point of origin. For the project, we considered only path-loss in an open-air environment. Using the path-loss equation, we estimated the distance between the point of origin for the SOI and BSs. In general, the free-space path loss (FSPL) equation is given as

$$P = 20 \log_{10} \left(\frac{4\pi x}{\lambda} \right)$$

EQUATION 1: GENERAL FREE-SPACE PATH-LOSS EQUATION (FSPL), IN DECIBELS.

where P denotes the path-loss in decibels, x is the distance from the reference point (the receiver station) to the target, and λ is the wavelength of the signal. Since the system estimates distance, x, Equation 1 is rearranged to

$$x = \frac{\lambda}{4\pi} 10^{P/20}.$$

EQUATION 2: FSPL EQUATION REARRANGED TO SOLVE FOR DISTANCE PARAMETER.

While theoretically Equation 1 holds true in a real-word situation, it may not be accurate due to atmospheric effects (precipitation, humidity, altitude, temperature, etc.) and environmental effects (vegetation, proximity to objects, geographical topology, etc.). In order to estimate distances as accurately as possible, the system derived its own curve-fitted FSPL equation. Using the same mathematical steps shown in Equation 1 and Equation 2, the system estimated the distance from the receiver station to the target using curve-fitted, path-loss equation unique to each BS.

In order to derive an equation that related power and distance, a consistent method to profile the power at known distances was required. The method was required to be precise, but not necessarily accurate (as the distances were already known). A precise method was found by taking a complex (IQ) sample of the signal at a specific point (0 Hz, after the signal was brought back down to baseband). To estimate power, or more accurately the received signal strength indicator (RSSI) as the power level is specific to the software used to interface with the USRP, the magnitude squared of the IQ sample was utilized. Furthermore, this value was averaged (over 240,000 samples) to smooth out instantaneous fluctuations. Figure 2 shows a sample GFSK signal (smoothed using a weighted average) and the corresponding RSSI value, shown in the upper right corner, is 5.3×10^{-6}. It was decided that the system precision would be to two significant digits.

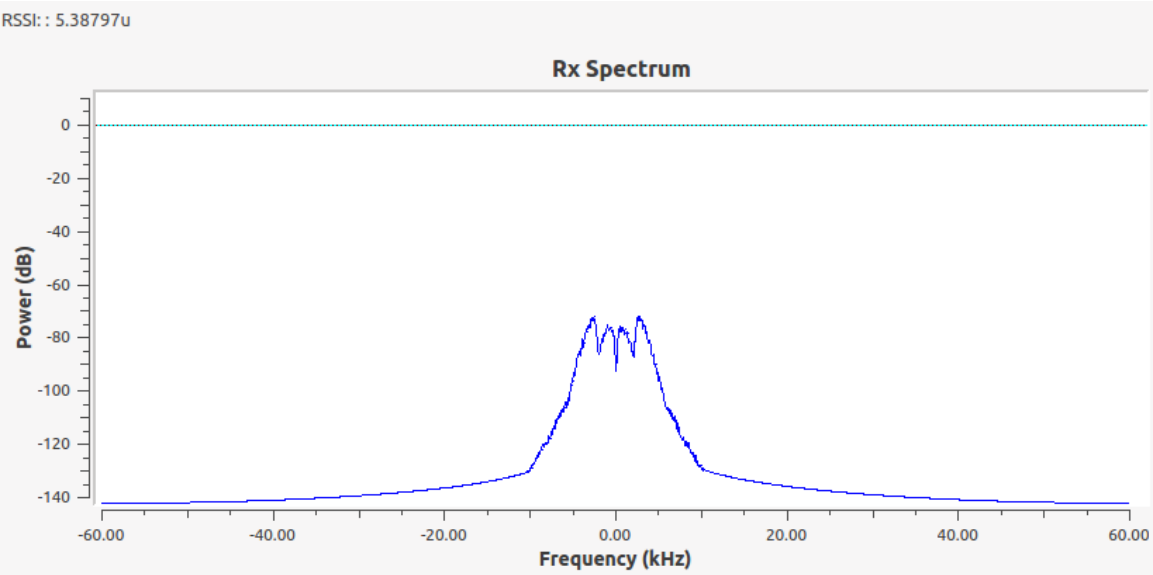

FIGURE 2: SAMPLE GFSK SIGNAL, AVERAGED, WITH CORRESPONDING AVERAGED RSSI VALUE.

By utilizing RSSI, sampling bias associated with individual hardware components of different receiver stations was factored out. Additionally, as each receiver station profiled power individually, biases associated with environmental factors (weather and geography) were also reduced.

Using the averaged power, a curve-fitted power-loss equation was derived and subsequently inverted to estimate distances using RSSI. To generate the path-loss model, the signal power was profiled at several fixed locations. The resulting data was fitted to an exponential curve. Figure 3 shows curve-fitted, path-loss equations based on real-world measurements from the three BSs, named RX 1, RX 2, and RX 3 respectively. The power values were scaled up by a factor of 10^6, resulting in a prototype function (Equation 3) where power, P, is a function of the distance, x.

$$P(x) = A \cdot e^{-b \cdot x}$$

EQUATION 3: EXPONENTIAL PATH-LOSS PROTOTYPE FUNCTION.

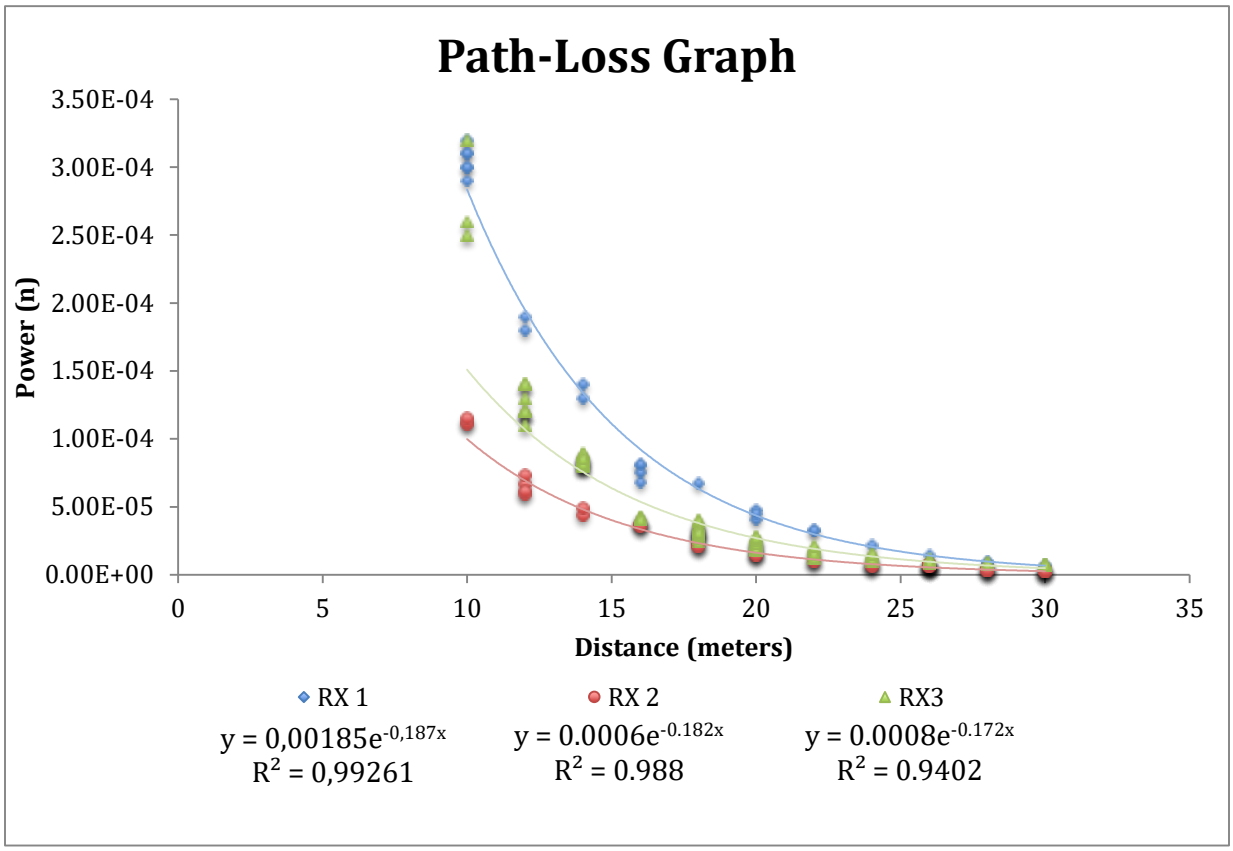

FIGURE 3: CURVE-FITTED PATH-LOSS EQUATIONS, BASED ON EXPONENTIAL REGRESSION, FOR THREE BASE STATIONS.

Internal biases from the receiver station hardware in addition to environmental biases caused significant variation in the A parameter obtained for each BS. The b parameter, however, appeared to be more consistent. Despite the effort put into determining the extent to which this variation was caused by environmental factors or hardware biases, no founded conclusion was derived. Hence, the analysis suggested that each receiver station profiled a characteristic path-loss equation of its own. Once the equations were derived, the inverse was found by inverting Equation 3, yielding

$$x = -\frac{1}{b}\ln\left(\frac{P}{A}\right).$$

EQUATION 4: INVERTED PROTOTYPE PATH-LOSS FUNCTION.

Equation 4 was used to estimate the positions of targets from receiver stations based on power data.

To estimate the distance between the point of origin for the SOI and the observation point at the BS, trilateration was employed. This is a mathematical technique used to determine relative location by utilizing absolute distances surrounding the observation point to create an area where the estimated point of origin resides, drawn by the intersection of the circles from all observation points. Two-dimensional trilateration was used, as it was assumed distance traveled in the Z

direction would be minimal compared to the X and Y directions. Additionally, three-dimensional trilateration would require at least four observation points, and increased computational complexity. The circular equation for two-dimensional trilateration are

$$d_n^2 = (x - x_n)^2 - (y - y_n)^2$$

EQUATION 5: DISTANCE EQUATION FOR N-TH OBSERVATION POINT TO THE INTERSECTION POINTS BETWEEN TWO OBSERVATION POINTS.

$$d_r^2 = (x_n - x_m)^2 + (y_n - y_m)^2,$$

EQUATION 6: DISTANCE BETWEEN N-TH AND M-TH OBSERVATION POINTS.

Using Equation 5 and Equation 6 results in the coordinates for the intersection points between observation points n and m, with the third observation point labelled as p, given in Equation 7 and Equation 8

$$x_{nm} = \frac{x_n + x_m}{2} + \frac{(x_m - x_n)(d_p^2 - d_n^2)}{2d_r^2} \pm \frac{y_m - y_n}{2d_r^2} \sqrt{\left((d_p + d_n)^2 - d_r^2\right)\left(d_r^2 - (d_p - d_n)^2\right)},$$

EQUATION 7: X-COORINDATE FOR INTERSECTION POINT OF CIRCLES BETWEEN N-TH AND M-TH OBSERVATION POINTS.

$$y_{nm} = \frac{y_n + y_m}{2} + \frac{(y_m - y_n)(d_p^2 - d_n^2)}{2d_r^2} \mp \frac{x_m - x_n}{2d_r^2} \sqrt{\left((d_p + d_n)^2 - d_r^2\right)\left(d_r^2 - (d_p - d_n)^2\right)}.$$

EQUATION 8: Y-COORDIANTE FOR INTERSECTION POINT OF CIRCLES BETWEEN N-TH AND M-TH OBSERVATION POINTS.

Using all combination of pairs of observation points, six coordinates are generated, depicting the intersection points that can be seen in Figure 4. Three points are eliminated (the intersection point between two circles that is furthest from the center of the third circle) to find the three points that result in the intersecting area of all three circles.

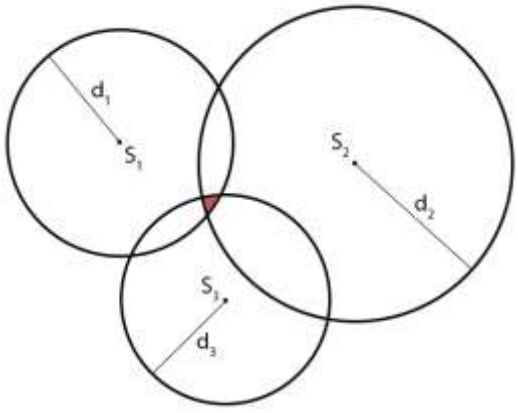

FIGURE 4: INTERSECTION POINTS FOR THREE BASE STATIONS, WITH THE ESTIMATED AREA OF ORIGIN FOR THE SOI COLORED IN RED.

The midpoint of the three intersection points is found to achieve the final coordinates, (X, Y), of the SOI shown in Equation 9 and Equation 10.

$$X = \frac{x_{nm}+x_{np}+x_{mp}}{3},$$

EQUATION 9: X-COORINDATE OF ESTIMATED POINT OF ORIGIN FOR THE SOI.

$$Y = \frac{y_{nm}+y_{np}+y_{mp}}{3}.$$

EQUATION 10: Y-COORDINATE OF ESTIMATED POINT OF ORIGIN FOR THE SOI.

RESULTS

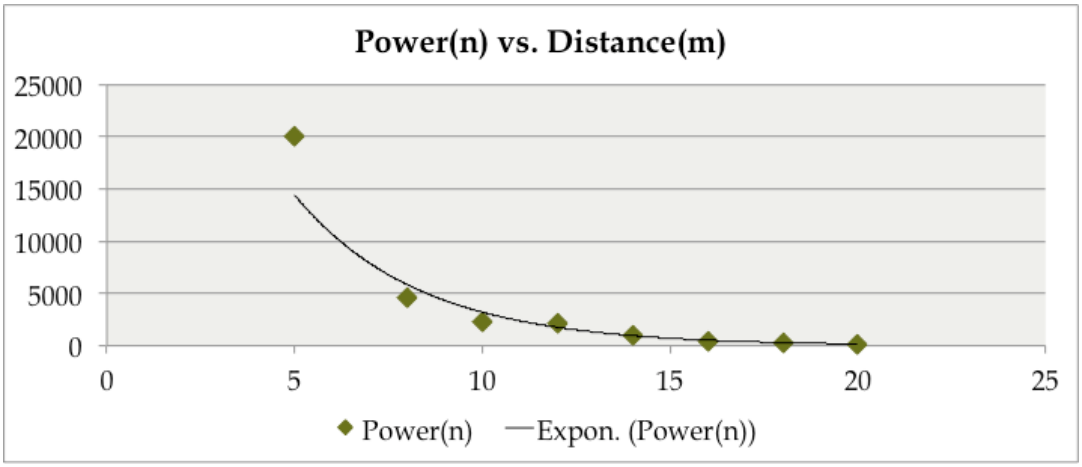

FIGURE 5: EXAMPLE PATH-LOSS EQUATION.

Figure 5 shows an example path loss curve with the corresponding equation

$$P = 64817e^{-0.301x}.$$

EQUATION 11: PATH-LOSS EQUATION FOR FIGURE 5.

Inverting Equation 11 allows for an estimation of distance, shown in

$$x = -\frac{1}{0.301}\ln\left(\frac{P}{64817}\right)$$

EQUATION 12: DISTANCE ESTIMATION FORMULA DERIVED FROM EQUATION 11.

Table 1, Table 2, and Table 3 show the actual and estimated distances using the path-loss equations shown in Figure 3.

Actual Distance (m)	Estimated Distance (m)	Absolute Error (m)
10	9.72	0.28
12	12.66	0.66
14	14.42	0.42
16	17.30	1.30
18	18.46	0.46
20	20.61	0.61
22	21.72	0.28
24	24.00	0.00
26	26.06	0.06
28	28.13	0.13
30	30.13	0.13

TABLE 1: ACTUAL AND ESTIMATED DISTANCES USING PATH-LOSS EQUATION FOR BASE STATION RX 1.

Actual Distance (m)	Estimated Distance (m)	Absolute Error (m)
10	9.27	0.73
12	11.55	0.45
14	13.88	0.12
16	15.55	0.45
18	18.58	0.58
20	20.79	0.79
22	22.60	0.60
24	24.95	0.95
26	24.61	1.39
28	28.54	0.54
30	30.45	0.45

TABLE 2: ACTUAL AND ESTIMATED DISTANCES USING PATH-LOSS EQUATION FOR BASE STATION RX 2.

Actual Distance (m)	Estimated Distance (m)	Absolute Error (m)
10	7.04	2.96
12	11.30	0.70
14	13.65	0.35
16	17.39	1.39
18	18.59	0.59
20	21.42	1.42
22	23.37	1.37
24	25.56	1.56
26	26.68	0.68
28	26.84	1.16
30	27.59	2.41

TABLE 3: ACTUAL AND ESTIMATED DISTANCES USING PATH-LOSS EQUATION FOR BASE STATION RX 3.

As shown in the above tables, barring outliers, the path-loss model is accurate within 2 meters. Assuming that the absolute error does not rise beyond that, the prototype system is capable of

estimating the location of a SOI within a 2 m^2 area over roughly 450 m^2 coverage area. Assuming this ratio, however, the system does not scale well. For instance, with a 1000 km^2 area (and assuming that the collars could transmit a signal with enough power), the system would only be able to estimate the location of an SOI to within a 4.5 km^2 area. This issue can be circumnavigated by deploying BSs in a grid pattern over the entire are of interest, such that the area covered by any particular cell (the smallest area of coverage by a subset of BSs) is within a specific value.

It was also found that near the antenna for a BS, power readings were inconsistent. The distance surrounding the BS corresponded roughly to the near field region of the antenna, implying that the system as a minimum distance specification.

Additionally, at different distance segments from the BSs, the curve-fitted path loss models behaved differently. Observations led to the conclusion that close to the BSs, the data could be modelled exponentially, while farther away from the BS, the data became flatter. It was theorized that this was an artifact of exponential regression model that was used, as a pose to the base-10 logarithm that the FSPL equation (Equation 1) uses. Plotting $\ln x$ and $\log_{10} x$ shows that the base-10 logarithm behaved closer to the observed far distances.

CONCLUSION

Overall, the system was a proof of concept that proved utilizing a radio propagation model was acceptable given a location accuracy of 2 m^2. Using the radio propagation models and power data from the base stations enabled the use of trilateration to plot the estimated area of the collar location. The system proved that a cost-effective tracking system could be implemented with an initial investment in the BSs with the full system requiring low periodic maintenance primarily for retrieving data and replacing batteries, as well as low cost in terms of the collars.

The data presented in this paper was taken over an eight hour period in an open air grassy, environment. Atmospheric conditions were dry with temperatures ranging from roughly 75 °F to 90 °F. While these conditions are typical to the environment the data was taken in, real-world conditions are unlikely to be so stable. This implies that an empirical radio propagation model has a lifetime before it needs to be recalculated. This can be achieved by profiling the power between BSs (which are at known locations) in the area of coverage in a periodic manner.

The propagation model calculation can be automated if the system has a large number of BSs. The data presented in this paper shows that with twelve BSs, a location accuracy of 2m^2 is achievable. Increasing the number of BSs, and thusly the number of points in the model, will aid in increasing the accuracy of the system.

REFERENCES

[1] Lathi, B., & Ding, Z. (2009). Principles of Digital Data Transmission. In *Modern Digital and Analog Communication Systems* (4.th ed.). New York: Oxford University Press.

[2] Haykin, S. (2014). Signaling over AWGN Channels. In *Digital Communication Systems* (pp. 375-382). Hoboken, N.J.: Wiley.

[3] Pozar, D. (2012). Microwave Filters. In *Microwave Engineering* (4th ed.). Hoboken, NJ: Wiley.

[4] Balanis, C. (2005). Fundemental Parameters of Antennas. In *Antenna Theory: Analysis and Design* (3rd ed., pp. 94-96). Hoboken, NJ: Wiley Interscience.

[5] Ulaby, F., & Michielssen, E. (2010). Transmission Lines. In *Fundamentals of Applied Electromagnetics* (6th ed., pp. 51, 87-110). Boston: Prentice Hall

[6] Azevedo, J., & Santos, F. (2011). An Empirical Propagation Model for Forest Environments at Tree Trunk Level. *IEEE Transactions on Antennas and Propagation, 59*(6), 2357-2367. Retrieved December 6, 2014, from IEEE Xplore.

[7] Meng, Y., Lee, Y., & Ng, B. (2009). Empirical Near Ground Path Loss Modeling in a Forest at VHF and UHF Bands. *IEEE Transactions on Antennas and Propagation,* 1461-1468.

[8] Fcc.gov, (2014). *Multi-Use Radio Service (MURS)*. Retrieved 6 December 2014, from http://www.fcc.gov/encyclopedia/multi-use-radio-service-murs-0